AGU PUBLICATIONS

Geophysical Research Letters

RESEARCH LETTER
10.1002/2015GL065539

Key Points:
- The SST in the northwestern Mediterranean Sea depended on ice sheet and insolation
- Ice sheet influence was transmitted via cold northwesterly winds
- At glacial stages the amplitude of millennial-scale SST had a strong insolation component

Supporting Information:
- Texts S1 and S2 and Figures S3 and S4

Correspondence to:
A. Cortina,
acortina@usal.es

Citation:
Cortina, A., F. J. Sierro, J. A. Flores, B. Martrat, and J. O. Grimalt (2015), The response of SST to insolation and ice sheet variability from MIS 3 to MIS 11 in the northwestern Mediterranean Sea (Gulf of Lions), *Geophys. Res. Lett.*, *42*, 10,366–10,374, doi:10.1002/2015GL065539.

Received 3 AUG 2015
Accepted 19 NOV 2015
Accepted article online 24 NOV 2015
Published online 11 DEC 2015

The response of SST to insolation and ice sheet variability from MIS 3 to MIS 11 in the northwestern Mediterranean Sea (Gulf of Lions)

Aleix Cortina[1], Francisco Javier Sierro[2], José Abel Flores[2], Belen Martrat[1], and Joan O. Grimalt[1]

[1]Department of Environmental Chemistry, IDAEA-CSIC, Barcelona, Spain, [2]Department of Geology, University of Salamanca, Salamanca, Spain

Abstract Here we present a sea surface temperature (SST) record based on the $U^{k'}_{37}$ index from the PRGL1 borehole (Promess1) drilled on the upper slope of the Gulf of Lions (GL). This is the first continuous and high-resolution record in the northwestern Mediterranean Sea from marine oxygen isotope stage 3 (MIS) 3 to MIS 11. Due the location of the GL, the SST proxy can be considered to be a reliable tool to study the climate link between high latitude and midlatitude. During glacial inceptions, the northern ice sheet signal via cold northwesterly winds was first recorded in our study area in comparison with southern locations, highlighting the strong sensitivity of this location to high-latitude dynamics. Moreover, the amplitude of the millennial-scale variability in the western Mediterranean basin seems to be the result of both ice sheet and insolation variability.

1. Introduction

The Mediterranean is a relatively small, semienclosed basin surrounded by large continental masses with only one narrow connection to the Atlantic Ocean. Its climate is the consequence of the interaction between the atmosphere, marine processes, and topography [*Xoplaki et al.*, 2004]. Due to oceanographic processes taking place in the Gulf of Lions (GL), this is a key area to understanding the Mediterranean climate.

At present, sea surface temperature (SST) distribution and surface circulation are strongly affected by cold northwesterly winds [*Pinardi and Masetti*, 2000]. Some micropaleontological studies at PRGL1 [*Cortina et al.*, 2011, 2013] recorded an intensification of these winds during cold periods, causing increased mixing of the water column. *Kuhlemann et al.* [2008] produced for the Last Glacial Maximum (LGM) a Mediterranean synthesis of proxy data from sea surface to alpine latitudes. The SST data included foraminiferal [*Paul and Schäfer-Neth*, 2003; *Hayes et al.*, 2005] and alkenone-based [*Cacho et al.*, 2002] reconstructions, while alpine data comprised the equilibrium line altitude of glaciers and Paleoflora-based temperature [*Peyron et al.*, 1998; *Wu et al.*, 2007]. They reported an extraordinary cooling during LGM centered in the GL owing to more persistent northerly incursions of cold polar air, in agreement with climate model simulations [*Masson-Delmotte et al.*, 2006]. Accordingly, past SST changes in this region should have a strong signature derived from the intensity of the cold northwesterly winds that in turn depended on high-latitude dynamics. For this reason, and owing to its location, the GL is an excellent location to study the interconnection between high latitude and midlatitudes.

However, no long, continuous and high-resolution (i.e., centennial to millennial) records of SST are available for this region. In this study we provide the first continuous and high-resolution SST record, using the $U^{k'}_{37}$ index for the past four climatic cycles in the GL. Our main goal is to analyze this SST record, strongly influenced by continental air masses, and to compare it with other alkenone-based SST records located in the Alboran Sea [*Martrat et al.*, 2004] and the Iberian Margin [*Martrat et al.*, 2007], which are more influenced by oceanic conditions (e.g., transport of heat via the Atlantic Meridional Overturning Circulation (AMOC)), with the aim of investigating how high-latitude processes influenced northwestern Mediterranean basin conditions.

2. Regional Settings

The GL is situated in the northwestern part of the Mediterranean Sea. The general circulation is mainly driven by the Northern Current, which is divided into two branches: the main branch flowing through the open sea along the Catalan-Balearic Sea and the secondary branch, which circulates along the continental shelf edge

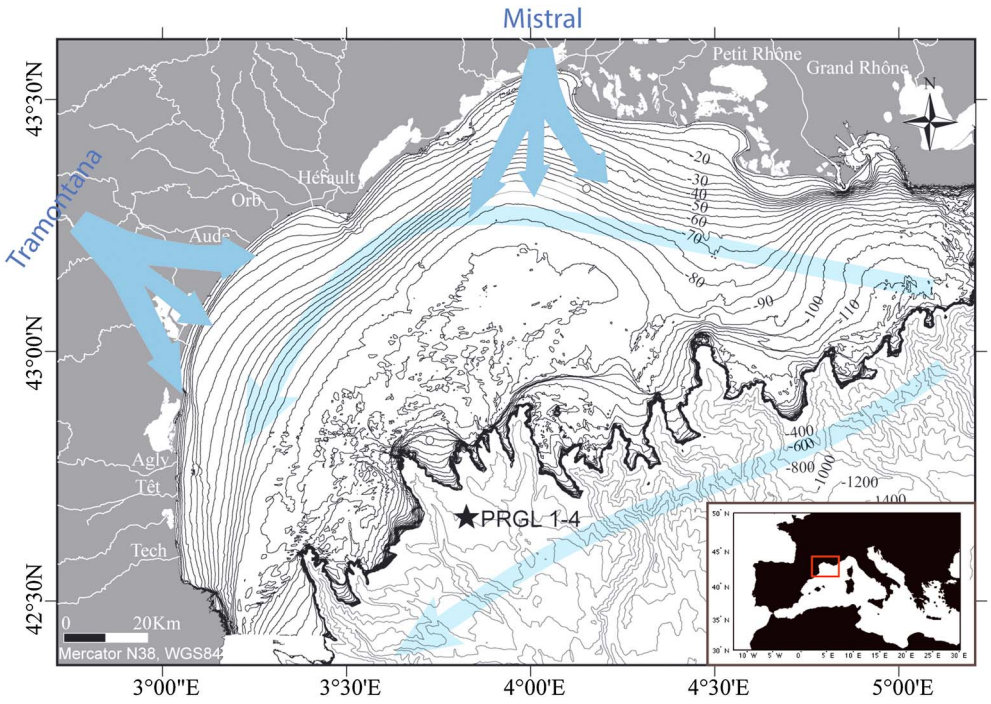

Figure 1. Map of the Gulf of Lions taken from *Jouet et al.* [2006]. Blue arrows represent the two North Current branches and the northwesterly winds. The PRGL1 is represented by a black star.

[*Millot*, 1990] (Figure 1). Owing to vertical mixing in winter and upwelling events, the GL is one of the most productive areas [*Lefèvre et al.*, 1997]. These events are principally driven by northwesterly winds (the Mistral and Tramontana), blowing through the Pyrenees, the Massif Central, and the Alps.

3. Material and Methods

We studied borehole PRGL1, drilled during the Promess1 campaign (summer 2004) in the GL (42.690 N, 3.838 E) (Figure 1) on the interfluve of the Boucart and Herault canyons at a water depth of 298 m. At the laboratory, 1 cm thick slices were taken every 10 cm. In this study we analyzed samples from 29 to 230 mbsf (meters below sea floor) covering from 29 kyr to 440 kyr.

From 29 to 157.10 mbsf, we used the age model published by *Sierro et al.* [2009]. For the second interval (from 157.10 to 230 mbsf) we used the age model published by *Frigola et al.* [2012]. In both cases, the age model was mainly based on a comparison of the *Globigerina bulloides* $\delta^{18}O$ record with the LR04 benthic stack [*Lisiecki and Raymo*, 2005], with the exception of the upper part, where the isotope record was tuned to Greenland ice cores.

3.1. SST Record

The SST record was based on the proportion of long chain diunsaturated and triunsaturated C_{37} alkenones. A total of 632 samples were analyzed. The biomarker sediment extraction procedure and SST calculation are detailed in Text S1 in the supporting information.

During glacial stages we evaluated the SST amplitude at millennial-scale level by means of standard deviation. The statistical procedure is detailed in Text S2, and the result was the StdT index (Standard deviation of SST after removing long-term variability) with high (low) values representing glacial stages with high (low) millennial-scale amplitude variability.

3.2. Spectral Analyses

Spectral analyses were performed with the REDFIT software [*Schulz and Mudelsee*, 2002] included in PAST 2.17b [*Hammer et al.*, 2001] using a Lomb periodogram algorithm to calculate the power spectral density. In order to reduce noise, two equal segments were used and averaged to obtain the spectra. We also show

the first-order autoregressive model (AR (1)) and 90% statistical significance of peaks based on a parametric approach (chi-squared distribution).

4. Results

4.1. SST Record

The SST values ranged between 3.5°C and 18.2°C (Figure 2c). Most of the SST record showed a strong precessional component, corroborated by the spectral analysis, which revealed the 21 kyr peak as the only significant at 90% confidence (Figure 2e). Higher values were reached during MIS 11 (18.2°C) and MIS 5 (18.1°C), followed by MIS 7 (16.6°C) and MIS 9 (16°C), respectively. During these interglacial stages, temperatures exhibited sharp transitions between stadial and interstadial periods.

The lowest values were achieved during Termination IV (3.5°C). For the glacial stages that were recorded completely in this study, on average the lowest temperatures were reached during MIS 10 (6.4°C), followed by MIS 8 (8.7°C) and MIS 6 (10.5°C). The last glacial was not recorded completely, and its SST average of the period monitored (MIS 3 and MIS 4) was 8.7°C.

4.2. *G. bulloides* ^{18}O Record

The *G. bulloides* $\delta^{18}O$ record showed a similar (inverse) trend to the SST curve (Figure 2a). Both records only diverged in very specific time intervals. The most important feature was the slight $\delta^{18}O$ excursion at the beginning of MIS 6 (between 160 and 180 kyr). During this interval, temperatures were lower than those recorded in MIS 5e, while the isotope values were lower than for the MIS 5e period. Moreover, regarding the magnitude of both records, maximum isotope values were recorded during MIS 6. However, the SST record fell during MIS 10.

5. Discussion

5.1. SST Variability in the GL From MIS 3 to MIS 11

Site PRGL1 is situated in the upper slope of the GL where strong glacial/interglacial environmental changes have been reported due to sea level variability [*Sierro et al*., 2009] as monitored by strong differences in sedimentation rate (Figure 2b). During lowstands, Rhone's plume approaches, increasing the sediment and freshwater discharge. It has been suggested that alkenones from coastal areas receiving significant freshwater inputs are produced by organisms adapted to lacustrine sediments characterized by high concentration of the tetraunsaturated compound [*Cranwell*, 1985] decreasing the sensitivity of the U^k_{37} index to SST [*Conte et al*., 1994; *Ficken and Farrimond*, 1995]. However, our SST data seem unaffected by river discharge since tetraunsaturated compound is almost absent in significant concentrations throughout the entire record. Moreover, the $\delta^{18}O$ record does not show the anomalous negative values (Figure 2a) typical of freshwater discharge environments in the Mediterranean [*Sierro et al*., 2005], and neither planktonic nor benthic foraminifer show the typical low-salinity species during MIS 6, MIS 8, and MIS 10 [*Cortina et al*., 2013].

The location of the GL in the northern margin of the Mediterranean plays an important role in seasonal SST variability. Currently, SST and ocean circulation in the western Mediterranean are strongly affected by northwesterly winds [*Pinardi and Masetti*, 2000]. This atmospheric pattern produces the frequent upwelling of cold waters [*Millot*, 1982], causing a strong SST interannual variability that ranges from 19°C in summer to 13°C in winter. Furthermore, current organic carbon productivity, including alkenones, largely peaks in winter and spring, coinciding with the upwelling of cold waters [*Rigual-Hernández et al*., 2013]. Considering both the influence of the cold northwesterly winds and the spring-winter signature, the SST records obtained in the GL show a colder imprint in comparison with other SST records situated at southern locations, producing a north-south temperature gradient. In particular, SST records in the Alboran Sea [*Martrat et al*., 2004] and the Iberian Margin [*Martrat et al*., 2007] are more related to both spring-summer conditions and a stronger influence of warmer waters (via AMOC) [*Heburn and La Violette*, 1990]; and hence, warmer SSTs are recorded. A strong SST gradient between the GL and the Alboran Sea was found, reaching values of 10°C during MIS 6 and 12.5°C during MIS 5e. A previous study based on planktic foraminiferal assemblages [*Hayes et al*., 2005] quantified this gradient around 5°C during LGM. These data suggest that cold northwesterly winds had a major impact in the upper slope of the GL, making this place suitable for monitoring their intensity.

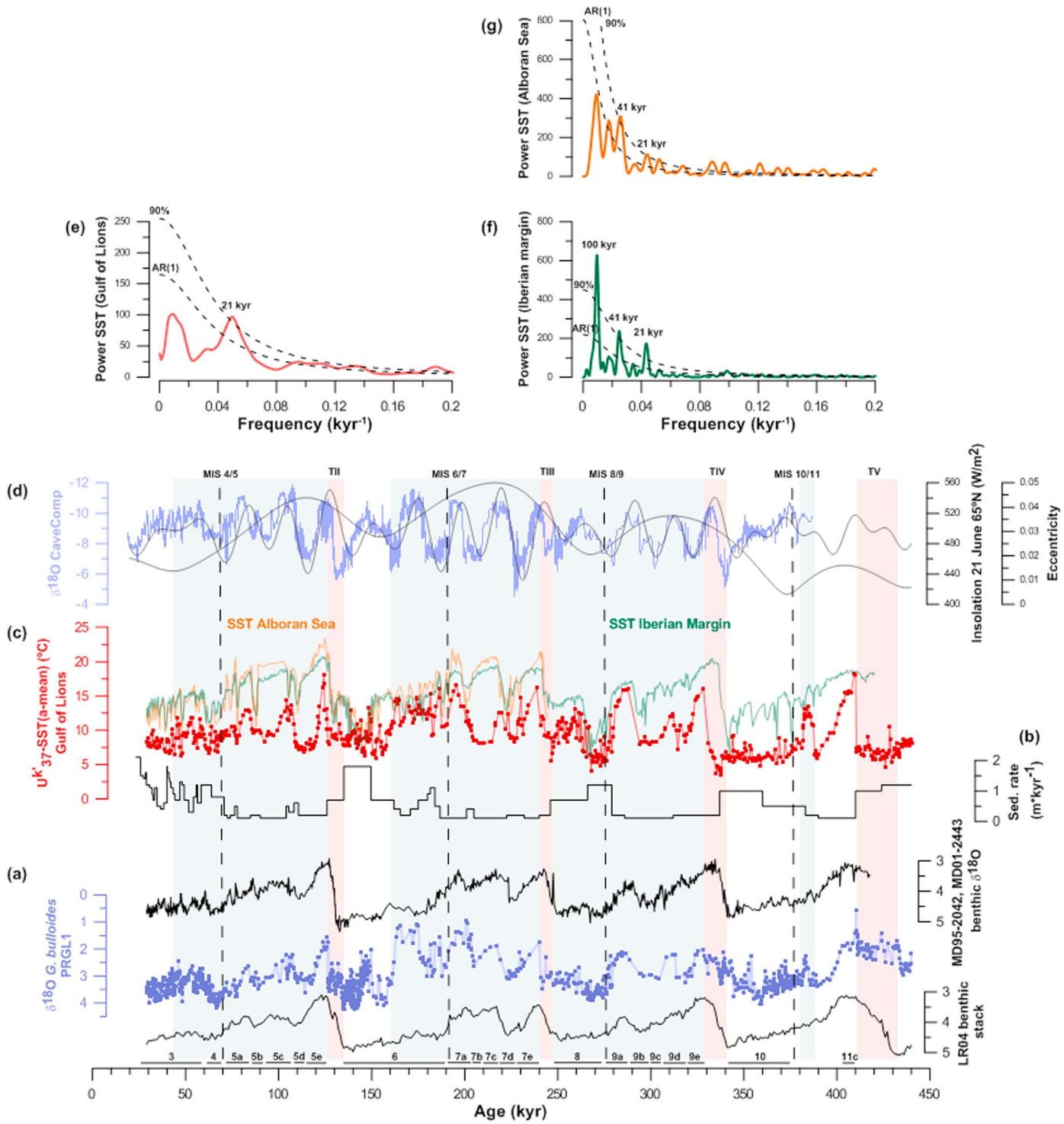

Figure 2. Climate variability from MIS 3 to MIS 11. (a) $\delta^{18}O$ isotope profiles. In the Gulf of Lions, we used $\delta^{18}O$ from *G. bulloides* [*Sierro et al.*, 2009; *Frigola et al.*, 2012]. LR04 benthic stack [*Lisiecki and Raymo*, 2005]. The benthic $\delta^{18}O$ profiles in cores MD95-2042 and MD01-2443 [*Shackleton et al.*, 2000; *Tzedakis et al.*, 2004; *de Abreu et al.*, 2005; *Martrat et al.*, 2007]. (b) Sedimentation rate (m*kyr^{-1}). (c) SST profiles from the Gulf Lions, Alboran Sea [*Martrat et al.*, 2004], and Iberian Margin [*Martrat et al.*, 2007]. (d) Composite Speleothem Record (CaveComp) [*Caballero-Gill et al.*, 2012]. Insolation (21 June, 65°N) and eccentricity [*Laskar et al.*, 2004]. Power spectral analysis of SST in (e) the Gulf of Lions, (f) the Alboran Sea, and (g) Iberian Margin. Dashed line represents first-order autoregressive model (AR(1)) and 90% significance of peaks. Green bars represent periods with close correspondence between SST in the Gulf of Lions and CaveComp.

Spectral analysis (Figures 2e–2g) also unveils differences between northern and southern records. The SST in the GL is mainly driven by precession (Figure 2e) because of the strong influence of summer radiation on the annual mean heat budget in the Mediterranean. However, the minor dependence of southern records on North Hemisphere Summer Insolation (NHSI) is evident in their power spectra (Figures 2f and 2g) showing 100 kyr and obliquity (41 kyr) signals besides the precession imprint.

On the contrary, we also found a close correspondence during most of the record between GL SST and the Composite Speleothem Record (CaveComp) [*Caballero-Gill et al*., 2012] (Figure 2d) generated from data from three caves in southeastern China (Sambao, Linzhu, and Hulu) [*Wang et al*., 2001, 2008; *Cheng et al*., 2009]. This $\delta^{18}O$ record provides information about the precipitation and temperature in this area [*Caballero-Gill et al*., 2012] and has been considered to reflect changes in the intensity of the East Asian Monsoons (EAM) [*Wang et al*., 2008]. This correspondence (green bars Figure 2) is due to the common link of both records to NHSI. Although GL SST record has a spring-winter imprint, higher values will be irremediably associated to high NHSI that drives EAM. During interglacial stages, maximum (minimum) NHSI at the precession band was linked to both high (low) values of SST in the GL and the intensity of the EAM in southeastern China, assuming an average lag of 4.8 kyr between insolation forcing and the SST response [*Lisiecki and Raymo*, 2005]. However, during glacial stages, this relationship weakened. Hence, in these stages the effect of insolation dampened in the GL in comparison with monsoon intensity, in particular during MIS 10, the end of the MIS 3, and—to a lesser extent—during MIS 6.

This lack of correspondence during glacial stages could be caused by the stronger influence of the Northern Hemisphere Ice Extent (NHIE) on the GL SST compared with EAM. On the northern Mediterranean margins, SST increases in the wake of higher summer radiation. However, during winter the decline in SST associated with the reduced insolation is enhanced by the heat losses linked to the cool winds flowing from northern latitudes as demonstrated by the stronger north-south SST gradient detected in our study compared with *Hayes et al*. [2005]. The link between the NHIE and the intensity of northwesterly winds has been demonstrated in previous studies [*Kuhlemann et al*., 2008; *Cortina et al*., 2011] that invoke a more southerly position of the polar front [*Pflaumann et al*., 2003] as a trigger for the frequent and/or persistent invasion of Arctic air masses. Therefore, in the GL the degree of dependence of SST on NHSI is more evident at times of high-amplitude changes in insolation but is more influenced by changes in the NHIE at times of low-amplitude oscillations in NHSI.

Our results are in agreement with the strength of glaciations as described by *Shackleton et al*. [1987]. MIS 10 corresponds to low NHSI and strong glaciations; and hence, there is no agreement with our record and EAM variability. By contrast, MIS 8 corresponds to high NHSI and low glacial conditions, accounting for the strong correspondence between both records. Due to the orbital configuration, the amplitude of insolation changes in MIS 6 is the highest among the glacials, although the SST did not increase in the same proportion and a weak correspondence with EAM was recorded. The main cause seems to be the extreme glaciation during the interval considered together with MIS 2 as the most extreme.

The results discussed in this section point to the high degree of dependence of the GL SST on the NHIE, making it a suitable tool for monitoring atmospheric connections between high latitude and midlatitude.

5.2. Rapid SST Response in the GL During Glacial Inceptions

Some previous research has pointed to the tight relationship between oceanic and atmospheric temperature at millennial-scale variability [*Sanchez-Goñi et al*., 2013]. Nevertheless, previous studies based on models [*Ruddiman and McIntyre*, 1981; *Risebrobakken et al*., 2007] suggest the existence of a thermal gradient between the ocean and the atmosphere during ice sheet growth. This scenario was finally corroborated by *Sanchez-Goñi et al*. [2013], demonstrating for the first time by means of marine and terrestrial paleoproxies a thermal ocean-atmosphere gradient that occurred at millennial-scale during the extensive ice sheet growth of the MIS 5a/MIS 4 transition.

As discussed in the previous section, the GL SST record is a reliable tool for monitoring NHIE dynamics via atmospheric teleconnections between high latitude and midlatitude. Furthermore, due to their location, the Alboran Sea [*Martrat et al*., 2004] and Iberian Margin [*Martrat et al*., 2007] SST records monitor changes in the transport of heat via the AMOC. Consequently, comparison of these three records should provide an idea of the degree of the coupling/decoupling between the ocean and the atmosphere during ice sheet

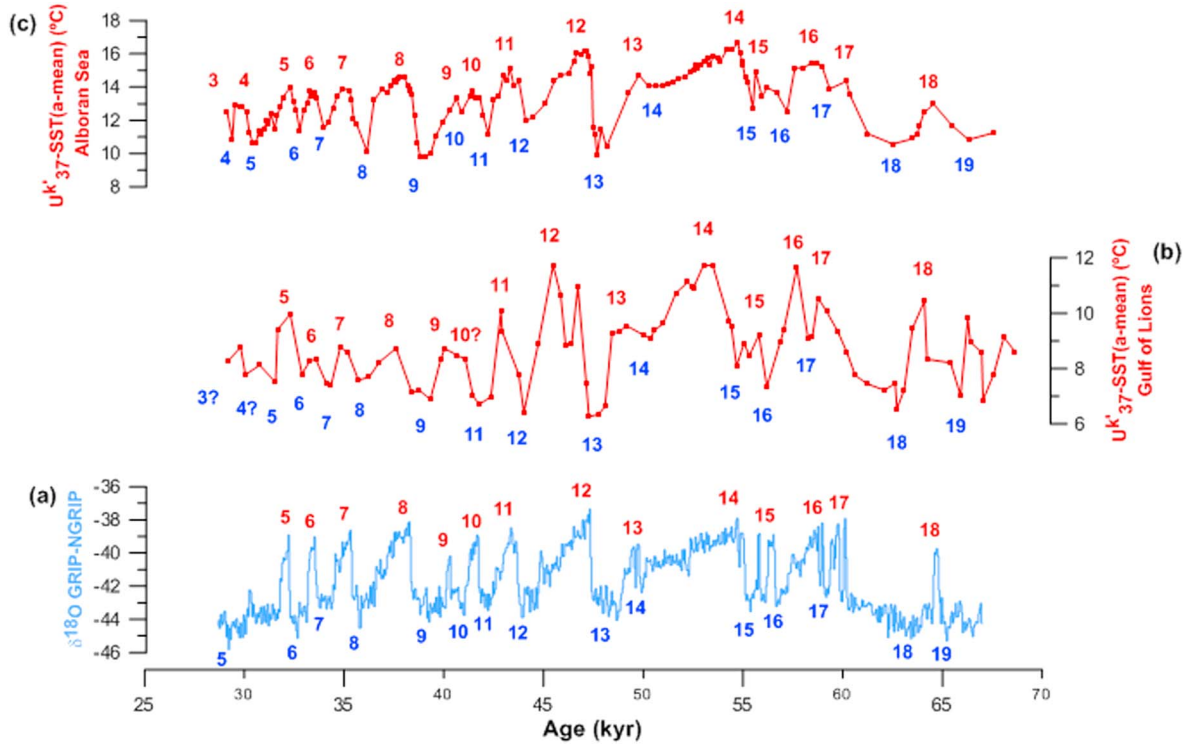

Figure 3. MIS 3 and MIS 4 climate variability. (a) δ^{18}O ice record in the North Greenland Ice Core Project. (b) SST in the Gulf of Lions. (c) SST in the Alboran Sea [*Martrat et al.*, 2004].

growth along the last 400 kyr (250 kyr in the case of the Alboran Sea record). Some age discrepancies can be observed between our record and southern Mediterranean records (Figure 2c), such as in MIS 9e and MIS 11c. This is due to a different isotope curve targeting when constructing age models, as demonstrated by isotope records (Figure 2a). Our age model is based on the LR04 benthic stack [*Lisiecki and Raymo*, 2005], while from the second to the fourth climate cycles, *Martrat et al.* [2007] used the Antarctica Dome C isotopic record in the edc2 age scale [*European Project for Ice Coring in Antarctica*, 2004; *Parrenin et al.*, 2004] as a target curve.

In our record, a prominent warming at the onset of interglacials was followed by a rapid decrease in temperature, while in the Iberian Margin and the Alboran Sea warmer temperatures persisted for longer. This pervasive behavior (e.g., 5e, 7c, 9e, and 11e) can clearly be seen in substage MIS 5e during the Eemien. A rapid cooling of the GL contrasted with relatively warm waters at the entrance of the Mediterranean or at the Iberian Margin. This suggests an early glacial inception of the Northern Hemisphere ice sheets, triggering cool winds toward the GL in winter, while Atlantic waters would have remained relatively warm. *Sanchez-Goñi et al.* [2013] propose that lower summer insolation at high latitudes, cooler landmasses, and enhanced AMOC [*Sanchez-Goñi et al.*, 2013] would have created an optimal configuration for rapid ice sheet growth, collecting moisture from the subpolar and northern subtropical Atlantic owing to its high heat content [*Ruddiman and Mcintyre*, 1979]. However, the control of high-latitude dynamics from low latitudes through obliquity has been also proposed [*Bosmans et al.*, 2015] highlighting the need of further research.

The fact that the north-south thermal gradient was better constrained just after the onset of the interglacials than during major ice sheet growth events is due to the heat content in the GL. At the beginning of the interglacials, the heat content was high and consequently the effect of cold northwesterly winds on SST was stronger. However, as SST decreased the thermal effect owing to cold northwesterly winds would have been less evident since SST already had low values. This characteristic confers our SST proxy with high sensitivity to small ice sheet changes and demonstrates the strong effect that glacial inception had on the western Mediterranean basin.

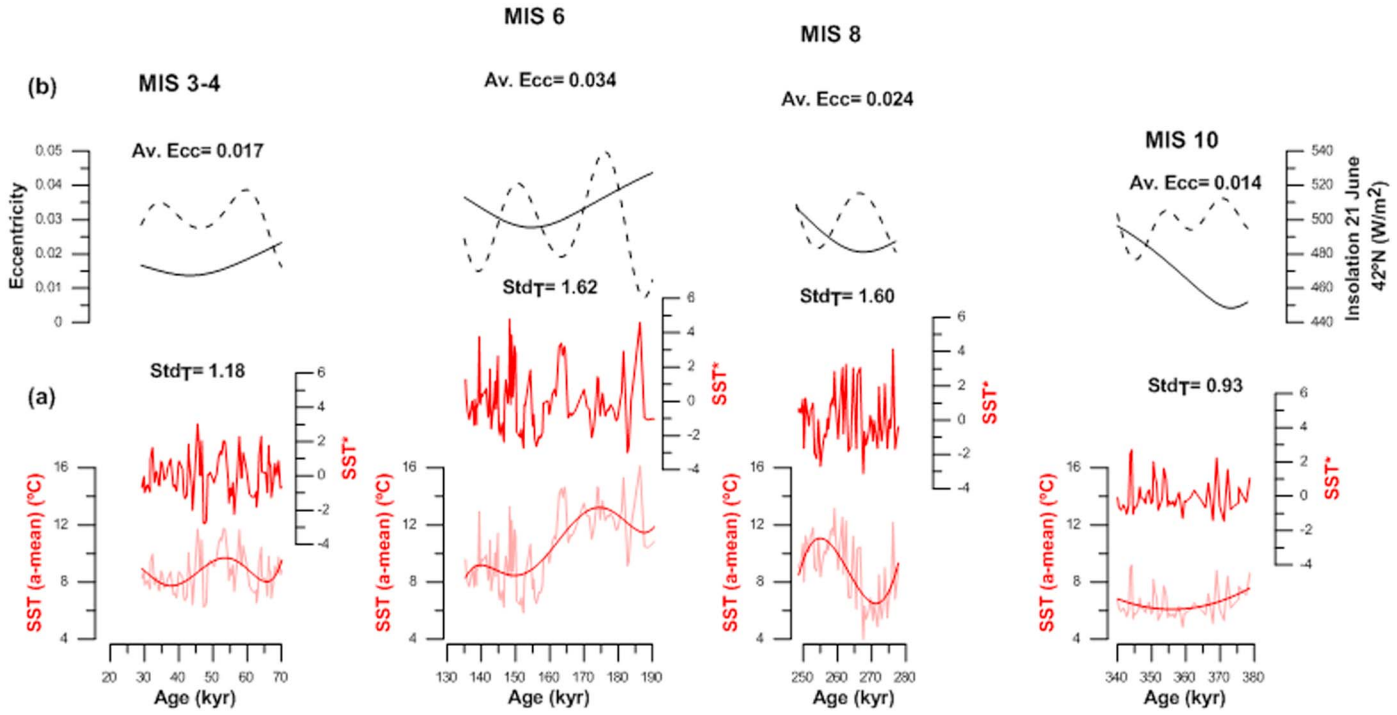

Figure 4. Millennial-scale SST variability in the Gulf of Lions during glacial stages. (a) At the bottom, the SST records and the polynomial that best fits long-term variability. Above SST*, which is the result of subtracting the polynomial fit from the original SST profile. StdT is the standard deviation of the SST* record. (b) Orbital parameters. Eccentricity and insolation (21 June, 42°N) [*Laskar et al.*, 2004].

Enhanced Western Mediterranean Deep Water (WMDW) formation in the GL driven mainly by northwesterly winds at times of stadial events has been proposed for the last glacial period [*Cacho et al.*, 2000]. This pattern contrast with low North Atlantic Deep Water (NADW) production, being this anticorrelation broken at times of Heinrich events [*Sierro et al.*, 2005]. Although WMDW formation does not take place at the location of PRGL1, our core site is in the path of northwesterly winds and records satisfactorily its intensity from MIS 6 to MIS 11 [*Cortina et al.*, 2013].

The enhancement of northwesterly winds has been recorded during glacial substages of MIS 7, MIS 9, and MIS 11 [*Cortina et al.*, 2013] when the NADW weakened. However, the high sensitivity of SST in the GL to northern ice sheet inception in comparison with southern locations could indicate an increase of WMDW production at times of warmer events in the Mediterranean basin, resulting in coupled WMDW and NADW productions between the colder and the warmer episodes during interglacials. This assuming a negligible effect of salinity in WMDW production that could be important at times of minimum precession and maximum obliquity [*Bosmans et al.*, 2015].

5.3. Millennial-Scale Variability Along Glacial Stages

Millennial-scale patterns recorded at high latitudes during MIS 3 and MIS 4 are also monitored in the GL by changes in SST (Figures 3a and 3b), demonstrating that alkenone-based SST estimation is a reliable proxy. However, the intensity of this variability differs from the SST changes recorded in the Alboran Sea [*Martrat et al.*, 2004] (Figure 3c), suggesting, as in the case of long-term variability, major atmospheric control.

In order to evaluate the millennial-scale amplitude of the SST, we used the StdT index. During MIS 3 and MIS 4, StdT decreased as ice volume increased (S3), in agreement with other studies that have related the amplitude of millennial-scale climate changes to the extension of the northern ice sheets [*Mcmanus et al.*, 1999; *Siddall et al.*, 2007]. However, on comparing the StdT index between glacial stages (Figure 4a), in the Mediterranean basin, the millennial-scale amplitude of the SST is not solely controlled by ice volume.

The most extreme glacials are MIS 6 and MIS 2, followed by MIS 10 and MIS 8 [*Shackleton*, 1987]. Therefore, assuming that larger ice volumes reduce millennial-scale variability amplitude, an inverse relationship

between the intensity of glaciations and the StdT index should be expected. Nevertheless, although we removed the long-term effect from our record, the StdT index has a strong nonlineal dependence on precession (Figure 4). The StdT linearly increased with precession amplitude until values of average eccentricity close to 0.025 (i.e., MIS 8). After that, high increases on average eccentricity produced low advances in StdT values (i.e., MIS 6). Hence, at millennial scale, the GL showed higher-SST amplitudes during glacial stages with higher precession amplitude.

We hypothesize that the dependence of millennial-scale variability on precession amplitude would have been the outcome of two opposite effects: the NHIE that precludes millennial-scale oscillations at times of larger ice volume, and the influence of NHSI, which tends to amplify it. Although during high-amplitude precession periods the higher and lower NHSI effects on SST should counteract each other, we suggest that only the higher NHSI values should be taken into account in order to explain the differential patterns of millennial-scale SST amplitude. The cooling effect of NHIE variability via northwesterly winds would have been enhanced at times of high NHSI because SST (heat content) would be higher and its decrease was more pronounced. By contrast, during low NHSI, the cooling effect triggered by a larger NHIE would have resulted in a less pronounced decrease of SST since this was already low (S4). Since millennial-scale variability is not only driven by NHSI but depends on two independent mechanisms operating at different scales, we would not expect a high-SST amplitude variability only linked with high NHSI values, since an increase in the NHIE could buffer SST oscillations for long periods of time. However, an increase in precession amplitude, and consequently higher values of NHSI, would have increased the probability of higher-SST amplitudes.

6. Conclusions

The strong NHSI dependence of SST is first corroborated by the power spectral analysis, which shows a predominant 21 kyr periodicity, and then by its similar behavior when compared with the intensity of the EAM, both increasing at times of precession minima. However, the sensitivity of the SST to precession would have been dampened during episodes of strong NHIE, probably as a consequence of more intense cold northwesterly wind episodes. The possibility of recording both middle and high-latitude effects simultaneously provides new insight into the climate processes from MIS 3 to MIS 11.

At glacial inceptions, the northwestern Mediterranean SST record reveals a sharper decrease when compared with the Alboran Sea and Iberian Margin SST records. This would have been the result of the continental imprint in our data and corroborates the idea of a thermal gradient between the cold continent and the warm ocean during events of ice sheet growth over the past 440 kyr.

Finally, millennial-scale SST amplitude increased during glacial stages with higher precession amplitudes. We hypothesize that the cooling/warming periods owing to the intensification/weakening of the northwesterly winds driven by NHIE dynamics would have been more pronounced at times of higher NHSI values. Consequently, prolonging the periods with higher NHSI would increase the probability of major SST increases/decreases.

Acknowledgments
Two anonymous reviewers are greatly acknowledged for their comments that improved the final version of this manuscript. This work was funded by GRACCIE project (CONSOLIDER-INGENIO CSD 2007–00067) and by the Formación de Personal Investigador (FPI) grant BES-2007-17602. Supporting data available at http://doi.pangaea.de/10.1594/PANGAEA.854682

References

Bosmans, J. H. C., F. J. Hilgen, E. Tuenter, and L. J. Lourens (2015), Obliquity forcing of low-latitude climate, *Clim. Past Discuss.*, *11*(1), 221–241.

Caballero-Gill, R. P., S. C. Clemens, and W. L. Prell (2012), Direct correlation of Chinese speleothem δ^{18}O and South China Sea planktonic δ18O: Transferring a speleothem chronology to the benthic marine chronology, *Paleoceanography*, *27*, PA2203, doi:10.1029/2011PA002268.

Cacho, I., J. O. Grimalt, F. J. Sierro, N. Shackleton, and M. Canals (2000), Evidence for enhanced Mediterranean thermohaline circulation during rapid climatic coolings, *Earth Planet. Sci. Lett.*, *183*(3–4), 417–429.

Cacho, I., J. O. Grimalt, and M. Canals (2002), Response of the Western Mediterranean Sea to rapid climatic variability during the last 50,000 years: A molecular biomarker approach, *J. Mar. Syst.*, *33–34*, 253–272.

Cheng, H., R. L. Edwards, W. S. Broecker, G. H. Denton, X. Kong, Y. Wang, R. Zhang, and X. Wang (2009), Ice Age terminations, *Science*, *326*(5950), 248–252.

Conte, M. H., A. Thompson, and G. Eglinton (1994), Primary production of lipid biomarker compounds by *Emiliania huxleyi*. Results from an experimental mesocosm study in Fjords of southwestern Norway, *Sarsia*, *79*(4), 319–331.

Cortina, A., F. J. Sierro, B. González-Mora, A. Asioli, and J. A. Flores (2011), Impact of climate and sea level changes on the ventilation of intermediate water and benthic foraminifer assemblages in the Gulf of Lions, off south France, during MIS 6 and 7, *Palaeogeogr. Palaeoclimatol. Palaeoecol.*, *309*(3–4), 215–228.

Cortina, A., F. J. Sierro, G. Filippelli, J. A. Flores, and S. Berné (2013), Changes in planktic and benthic foraminifer assemblages in the Gulf of Lions, off south France: Response to climate and sea level change from MIS 6 to MIS 11, *Geochem. Geophys. Geosyst.*, *14*, 1258–1276, doi:10.1002/ggge.20096.

Cranwell, P. A. (1985), Long-chain unsaturated ketones in recent lacustrine sediments, *Geochim. Cosmochim. Acta*, *49*(7), 1545–1551.

de Abreu, L., F. F. Abrantes, N. J. Shackleton, P. C. Tzedakis, J. F. McManus, D. W. Oppo, and M. A. Hall (2005), Ocean climate variability in the eastern North Atlantic during interglacial marine isotope stage 11: A partial analogue to the Holocene?, *Paleoceanography*, *20*, PA3009, doi:10.1029/2004PA001091.

European Project for Ice Coring in Antarctica (2004), Eight glacial cycles from an Antarctic ice core, *Nature*, *429*(6992), 623–628.

Ficken, K. J., and P. Farrimond (1995), Sedimentary lipid geochemistry of Framvaren: Impacts of a changing environment, *Mar. Chem.*, *51*(1), 31–43.

Frigola, J., et al. (2012), A 500 kyr record of global sea-level oscillations in the Gulf of Lion, Mediterranean Sea: New insights into MIS 3 sea-level variability, *Clim. Past*, *8*(3), 1067–1077.

Hammer, Ø., D. A. T. Harper, and P. D. Ryan (2001), Past: Paleontological statistics software package for education and data analysis, *Palaeontol. Electron.*, *4*(1), 9.

Hayes, A., M. Kucera, N. Kallel, L. Sbaffi, and E. J. Rohling (2005), Glacial Mediterranean sea surface temperatures based on planktonic foraminiferal assemblages, *Quat. Sci. Rev.*, *24*(7–9), 999–1016.

Heburn, G. W., and P. E. La Violette (1990), Variations in the structure of the anticyclonic gyres found in the Alboran Sea, *J. Geophys. Res.*, *95*(C2), 1599–1613.

Jouet, G., S. Berné, M. Rabineau, M. A. Bassetti, P. Bernier, B. Dennielou, F. J. Sierro, J. A. Flores, and M. Taviani (2006), Shoreface migrations at the shelf edge and sea-level changes around the Last Glacial Maximum (Gulf of Lions, NW Mediterranean), *Mar. Geol.*, *234*(1–4), 21–42.

Kuhlemann, J., E. J. Rohling, I. Krumrei, P. Kubik, S. Ivy-Ochs, and M. Kucera (2008), Regional synthesis of Mediterranean atmospheric circulation during the Last Glacial Maximum, *Science*, *321*(5894), 1338–1340.

Laskar, J., P. Robutel, F. Joutel, M. Gastineau, A. C. M. Correia, and B. Levrard (2004), A long-term numerical solution for the insolation quantities of the Earth, *Astron. Astrophys.*, *428*(1), 261–285.

Lefèvre, D., H. J. Minas, M. Minas, C. Robinson, P. J. L. Williams, and E. M. S. Woodward (1997), Review of gross community production, primary production, net community production and dark community respiration in the Gulf of Lions, *Deep Sea Res., Part II*, *44*(3–4), 801–832.

Lisiecki, L. E., and M. E. Raymo (2005), A Pliocene-Pleistocene stack of 57 globally distributed benthic d18O records, *Paleoceanography*, *20* PA1003, doi:10.1029/2004PA001071.

Martrat, B., J. O. Grimalt, C. Lopez-Martinez, I. Cacho, F. J. Sierro, J. A. Flores, R. Zahn, M. Canals, J. H. Curtis, and D. A. Hodell (2004), Abrupt temperature changes in the Western Mediterranean over the past 250,000 years, *Science*, *306*(5702), 1762–1765.

Martrat, B., J. O. Grimalt, N. J. Shackleton, L. de Abreu, M. A. Hutterli, and T. F. Stocker (2007), Four climate cycles of recurring deep and surface water destabilizations on the Iberian Margin, *Science*, *317*(5837), 502–507.

Masson-Delmotte, V., et al. (2006), Past and future polar amplification of climate change: Climate model intercomparisons and ice-core constraints, *Clim. Dyn.*, *26*(5), 513–529.

McManus, J. F., D. W. Oppo, and J. L. Cullen (1999), A 0.5-million-year record of millennial-scale climate variability in the North Atlantic, *Science*, *283*(5404), 971–975.

Millot, C. (1990), The Gulf of Lions' hydrodynamics, *Cont. Shelf Res.*, *10*(9–11), 885–894.

Parrenin, F., F. Rémy, C. Ritz, M. J. Siegert, and J. Jouzel (2004), New modeling of the Vostok ice flow line and implication for the glaciological chronology of the Vostok ice core, *J. Geophys. Res.*, *109*, D20102, doi:10.1029/2004JD004561.

Paul, A., and C. Schäfer-Neth (2003), Modeling the water masses of the Atlantic Ocean at the Last Glacial Maximum, *Paleoceanography*, *18*(3), 1058, doi:10.1029/2002PA000783.

Peyron, O., J. Guiot, R. Cheddadi, P. Tarasov, M. Reille, J.-L. de Beaulieu, S. Bottema, and V. Andrieu (1998), Climatic reconstruction in Europe for 18,000 YR B.P. from pollen data, *Quat. Res.*, *49*(2), 183–196.

Pflaumann, U., et al. (2003), Glacial North Atlantic: Sea-surface conditions reconstructed by GLAMAP 2000, *Paleoceanography*, *18*(3), 1065, doi: 10.1029/2002PA000774.

Pinardi, N., and E. Masetti (2000), Variability of the large scale general circulation of the Mediterranean Sea from observations and modelling: A review, *Palaeogeogr. Palaeoclimatol. Palaeoecol.*, *158*(3–4), 153–173.

Rigual-Hernández, A. S., M. A. Bárcena, R. W. Jordan, F. J. Sierro, J. A. Flores, K. J. S. Meier, L. Beaufort, and S. Heussner (2013), Diatom fluxes in the NW Mediterranean: Evidence from a 12-year sediment trap record and surficial sediments, *J. Plankton Res.*, *35*, 1109, doi:10.1093/plankt/fbt055.

Risebrobakken, B., T. Dokken, O. H. Otterå, E. Jansen, Y. Gao, and H. Drange (2007), Inception of the Northern European ice sheet due to contrasting ocean and insolation forcing, *Quat. Res.*, *67*(1), 128–135.

Ruddiman, W. F., and A. Mcintyre (1979), Warmth of the subpolar North Atlantic Ocean during Northern Hemisphere ice-sheet growth, *Science*, *204*(4389), 173–175.

Ruddiman, W. F., and A. McIntyre (1981), Oceanic mechanisms for amplification of the 23,000-year ice-volume cycle, *Science*, *212*(4495), 617–627.

Sanchez-Goñi, M. F., E. Bard, A. Landais, L. Rossignol, and F. d'Errico (2013), Air-sea temperature decoupling in western Europe during the last interglacial-glacial transition, *Nat. Geosci.*, *6*(10), 837–841.

Schulz, M., and M. Mudelsee (2002), REDFIT: Estimating red-noise spectra directly from unevenly spaced paleoclimatic time series, *Comput. Geosci.*, *28*(3), 421–426.

Shackleton, N. J. (1987), Oxygen isotopes, ice volume and sea level, *Quat. Sci. Rev.*, *6*(3–4), 183–190.

Shackleton, N. J., M. A. Hall, and E. Vincent (2000), Phase relationships between millennial-scale events 64,000-24,000 years ago, *Paleoceanography*, *15*(6), 565–569.

Siddall, M., T. F. Stocker, T. Blunier, R. Spahni, J. Schwander, J.-M. Barnola, and J. Chappellaz (2007), Marine isotope stage (MIS) 8 millennial variability stratigraphically identical to MIS 3, *Paleoceanography*, *22*, PA1208, doi:10.1029/2006PA001345.

Sierro, F. J., et al. (2005), Impact of iceberg melting on Mediterranean thermohaline circulation during Heinrich events, *Paleoceanography*, *20*, PA2019, doi:10.1029/2004PA001051.

Sierro, F. J., et al. (2009), Phase relationship between sea level and abrupt climate change, *Quat. Sci. Rev.*, *28*(25–26), 2867–2881.

Tzedakis, P. C., K. H. Roucoux, L. de Abreu, and N. J. Shackleton (2004), The duration of forest stages in Southern Europe and interglacial climate variability, *Science*, *306*(5705), 2231–2235.

Wang, Y., H. Cheng, R. L. Edwards, X. Kong, X. Shao, S. Chen, J. Wu, X. Jiang, X. Wang, and Z. An (2008), Millennial- and orbital-scale changes in the East Asian monsoon over the past 224,000 years, *Nature*, *451*(7182), 1090–1093.

Wang, Y. J., H. Cheng, R. L. Edwards, Z. S. An, J. Y. Wu, C. C. Shen, and J. A. Dorale (2001), A high-resolution absolute-dated Late Pleistocene monsoon record from Hulu Cave, China, *Science*, *294*(5550), 2345–2348.

Wu, H., J. Guiot, S. Brewer, and Z. Guo (2007), Climatic changes in Eurasia and Africa at the last glacial maximum and mid-Holocene: Reconstruction from pollen data using inverse vegetation modelling, *Clim. Dyn.*, *29*(2–3), 211–229.

Xoplaki, E., J. F. González-Rouco, J. Luterbacher, and H. Wanner (2004), Wet season Mediterranean precipitation variability: Influence of large-scale dynamics and trends, *Clim. Dyn.*, *23*(1), 63–78.